International Journal of Computational Research in Science and Technology
E-ISSN: 3108-0871, Volume 2 Issue 5
Sep-Oct 2026, PP 01-11

Investigation of Nanomaterials for High-Efficiency Energy Storage Devices

Md Javed[1], Mr Gorakh Waluba Gangurde[2]

[1](Research Scholar,
Department of Physics,
BRAB University,Muzaffarpur
research2phd13@gmail.com

[2](Assistant Professor
Department of Physics,
MVP Samaj's Karmveer Punjababa Govardhane Arts Commerce and Science College, Igatpuri, Dist-Nashik, Maharashtra
gangurdegorakh95@gmail.com)

Abstract. The efforts aimed at maximizing the efficiency of energy storage have led to detailed studies of nanoarchitectures of electrodes that address the kinetic and structural limitations of bulk materials. In this regard, the current research systematically explores the preparation, structural features, and electrochemical behavior of nanocomposites of graphene, MXenes, and transition metal oxides for supercapacitor and lithium-ion battery technologies. It was proposed to use the combination of hydrothermal and ex situ oxidative polymerization methods to synthesize $Ti_3C_2T_x$ MXenes/polyaniline and reduced graphene oxide/transition metal oxide nanocomposites. Cyclic voltammetry, galvanostatic charge-discharge, and impedance spectroscopy results have shown that MXene/PANI composites provide specific capacitance of more than 430 F g^{-1} with good cycling stability up to 10,000 cycles, while CoNiP/rGO nanocomposite electrodes demonstrate capacities close to 477 mAh g^{-1} with retention. Comparison of the studied systems with the reference carbon and oxide ones shows that nanoarchitectures where conductive scaffolds provide resistance to restacking of the structure, while redox-active components provide redox-active sites can be considered a solution.

Keywords: Nanomaterials, Mxene, Graphene, Supercapacitor, Lithium-Ion Battery, Nanocomposite Electrodes

I. Introduction

Global move towards the adoption of electrification of transport and renewable energy technologies has created huge challenges for electrochemical energy storage devices. While Li-ion batteries continue to dominate the scene when it comes to use of batteries in portable devices and electric vehicles, such batteries have intrinsic limitations when it comes to power density and cycle life that make them less suitable for high-frequency and high-power operations. Supercapacitors serve as a way around through their fast charge-discharge capacity but have low energy densities than the batteries. The solution to this challenge has been found in nanomaterials [1][6][7].

The inherent benefit of nanostructured electrodes is the significant boost in electrochemically active surface area per unit geometric surface area. In the case of electric double layer capacitors, the higher specific surface area results in increased charge storage capabilities in the electrode–electrolyte interface. In the case of pseudo-capacitive and battery materials, the reduced diffusion length of nanostructures results in faradic reactions that take place at an extremely fast rate comparable to

surface reactions. Carbon-based materials like graphene and carbon nanotubes have exhibited excellent electrical and mechanical properties and thus are considered ideal scaffold materials for composite electrodes [1][9]. The 2D MXenes, which are obtained by selective etching of MAX-phase precursors, have unique properties including metallic conductivity, hydrophilicity, and adjustable interlayer spacing and therefore make suitable candidates for use in aqueous electrolytes [2][3]. Transition metal oxides and phosphides have high theoretical capacity because of multi-electron redox reactions although they have low conductivity [6][8].

However, the rational design of such hybrid architectures that can take advantage of the synergetic effects is highly challenging. First, restacking of the two-dimensional flakes during the process of electrode preparation results in a dramatic reduction of the accessible surface area. Second, volume expansion of the conversion-type anodes brings about mechanical instability and capacity fading. Third, controllable and scalable synthesis of the composites with predictable electrochemical performance requires the precise control over nucleation, growth, and self-assembly steps [3][6][7]. This study aims at solving the problems mentioned above by studying the interdependence between the synthesis parameters, microstructure and electrochemical performance of the composites of three families of materials: MXenes/polyaniline [2], reduced graphene oxide-transition metal phosphides [1], and multi-component transition metal oxides/MXenes [8].

II. Literature Survey

In the case of the development of nanomaterial electrodes for energy storage devices, two directions have developed in parallel for supercapacitors and batteries, although the tendency to unite has become obvious recently [6][7]. The basic knowledge about electrical double layer capacitor energy storage has been gained from the study of carbon-based nanomaterials, which possess excellent electrical conductivity and thermal stability but whose actual capacitance is limited due to quantum capacitance and impossibility to preserve the exfoliated state of the material while producing the electrode [1][9]. Activated carbons produced from biomass are more economically viable, with precursors like coconut shell and rice husks providing specific surface areas in excess of 2000 m^2/g and capacitances up to 300-420 F/g in aqueous electrolyte [7].

The MXene family of materials represents an interesting contender for pseudocapacitive and battery-type electrodes [2][3]. Generally, MXene structures can be described using the formula of $M_{n+1}X_nT_x$, where carbides and nitrides of early transition metals constitute the basis of material. The most widely studied member of this family is represented by $Ti_3C_2T_x$ [2][3]. The conductive properties of MXene flakes and surface modifications, allowing for ion intercalation, facilitate the development of thick electrode designs with mass-dependent capacitance, rather than thin-film capacitors [2][3]. However, van der Waals forces lead to the restacking of individual delaminated layers, resulting in a decrease in accessible active sites and electrolyte access [2][3]. The use of conductive polymers, such as polyaniline, as an additive within MXene interlayers has demonstrated potential as an effective restacking mitigation technique with additional pseudocapacitance [2]. For example, a composite $Mo_2Ti_2C_3T_x$/PANI synthesized through the ex-situ oxidative polymerization process showed 563 F g^{-1} at 0.5 A g^{-1} with 95.15% retention after 1000 cycles [2].

The MXene family of materials represents an interesting contender for pseudocapacitive and battery-type electrodes [2][3]. Generally, MXene structures can be described using the formula of $M_{n+1}X_nT_x$, where carbides and nitrides of early transition metals constitute the basis of material. The most widely studied member of this family is represented by $Ti_3C_2T_x$ [2][3]. The conductive properties of MXene flakes and surface modifications, allowing for ion intercalation, facilitate the development of thick electrode designs with mass-dependent capacitance, rather than thin-film capacitors [2][3]. However, van der Waals forces lead to the restacking of individual delaminated layers, resulting in a decrease in accessible active sites and electrolyte access [2][3]. The use of conductive polymers, such as polyaniline, as an additive within MXene interlayers has demonstrated potential as an effective restacking mitigation technique with additional pseudocapacitance [2]. For example, a composite $Mo_2Ti_2C_3T_x$/PANI synthesized through the ex-situ oxidative polymerization process showed 563 F g^{-1} at 0.5 A g^{-1} with 95.15% retention after 1000 cycles [2].

The development of solid polymer electrolytes is another research direction that aims to produce safe batteries [4][10]. The combination of a poly(vinylidene fluoride) matrix with fluorinated silica nanoparticles as compatibilizers provided ionic conductivity of 2.7×10^{-4} S cm^{-1} at room temperature and stable cycling up to 500 cycles [4]. Another approach involved two-

International Journal of Statistics and Mathematical Research Trends
E-ISSN: 3108-0871, Volume 2 Issue 5
Sep-Oct 2026, PP 01-11

dimensional filler materials like LiC_3N_4 nanosheets embedded into poly(ethylene oxide) matrices; however, room-temperature conductivity has remained an open problem [10]. As a common trend in the literature on nanomaterials in battery applications can be traced, their performance is not determined solely by intrinsic characteristics, but rather by interface structures: between the active material and the conductive filler, between the electrode and the electrolyte, and between nanoscale components of composite materials [3][4][6].

III. Proposed Methodology

Materials and Reagents

MAX phase Ti_3AlC_2 (98%) powder and aniline (99.5%), ammonium persulfate (98%), hydrochloric acid (37%), hydrofluoric acid (48%), ferric nitrate nonahydrate, copper nitrate trihydrate, cobalt chloride, nickel nitrate hexahydrate, and sodium hypophosphite were all acquired from Sigma-Aldrich. Potassium hydroxide and deionized water (18.2 MΩ cm) were employed in the work. Nickel foam substrates (1 × 2 cm², 1.6 mm) were rinsed through a sonication process in acetone, ethanol, and distilled water before utilization.

Synthesis of $Ti_3C_2T_x$ MXene

$Ti_3C_2T_x$ MXene was delaminated through aluminum etching of MAX phase. First, 1 g of Ti_3AlC_2 powder was slowly mixed into 20 mL of 40% HF aqueous solution through magnetic stirring at ambient temperature. For 24 hours, etching took place. Then, washing through centrifugation (3500 rpm for 10 min) with deionized water was carried out several times until the supernatant reached pH ≈ 6. Next, multilayer MXene was dispersed in deionized water and sonicated under argon gas for 1 hour to obtain exfoliation of the material. Delaminated suspension was separated through centrifugation at 3500 rpm for 30 min and the supernatant containing single/few layer MXene was collected.

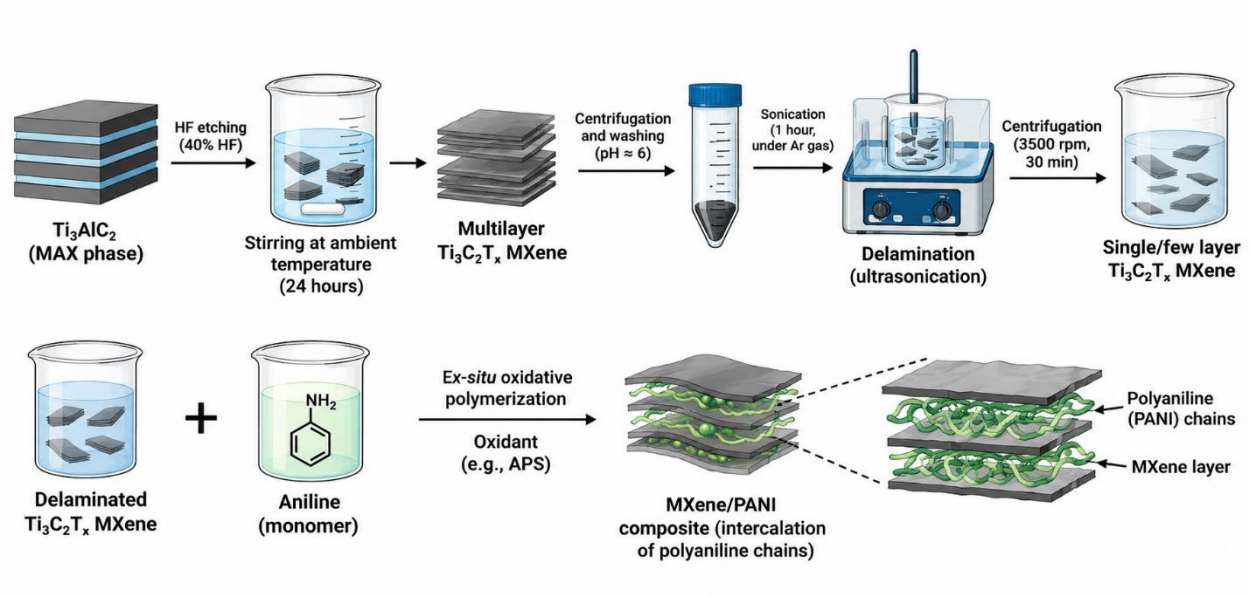


Figure 1: Schematic illustration of the synthesis procedure for $Ti_3C_2T_x$ MXene and MXene/PANI composite

The illustration shows the etching process of Al from Ti_3AlC_2 material using hydrofluoric acid, and then delamination of the etched material through ultrasonication to obtain MXene sheets. The next step is the oxidative polymerization of aniline in the presence of MXene to obtain MXene/PANI nanocomposite.

Synthesis of MXene/PANI Composite

The synthesis of the MXene/PANI composite was carried out via ex-situ oxidative polymerization using the protocol described recently in literature. First, the delaminated suspension of MXene (0.1 g equivalent) was sonicated in 10 mL of deionized water for 60 min. Then aniline (200 μL) was added to the MXene dispersion with magnetic stirring for 10 min. Second, 5 mL

of 1 M HCl was prepared separately and added to the MXene-aniline solution while the mixture was cooled in an ice bath (reaction temperature was kept close to 0°C). After reaching homogeneity, 200 mg of ammonium persulfate in 5 mL of deionized water was rapidly added to the reaction mixture to initiate the oxidative polymerization process. During the first 5 h of the process, the reaction mixture was kept in an ice bath to release the exothermic heat of the polymerization process. After that time, the reaction mixture was stirred at room temperature for 5 h to finish the polymerization process. The resulting dark-green precipitate was purified by several times washing with deionized water until the neutral pH of the wash water was achieved.

Synthesis of CoNiP/rGO Hybrid

The CoNiP/rGO nanocomposite was synthesized via a one-pot colloidal approach followed by electrophoretic deposition technique, which was a modification of the existing methodologies. Graphene oxide was prepared by modified Hummers' approach and then exfoliated in distilled water via sonication process. CoCl2 and NiCl2 in 1:1 ratio by moles were dissolved in the GO solution in presence of nitrogen gas. Sodium hypophosphite was used as a source of phosphorus and the whole solution was heated up to 110 °C under reflux for better nucleation and growth of CoNiP nanoparticles on GO sheets. The product obtained was isolated by centrifugation and was thoroughly washed with ethanol. Then the product was thermally reduced in argon atmosphere at 300 °C for 2 hours to get rGO. The electrodes were prepared by electrophoretic deposition of the CoNiP/rGO composite from an isopropanol solution at 50 V for 5 minutes.

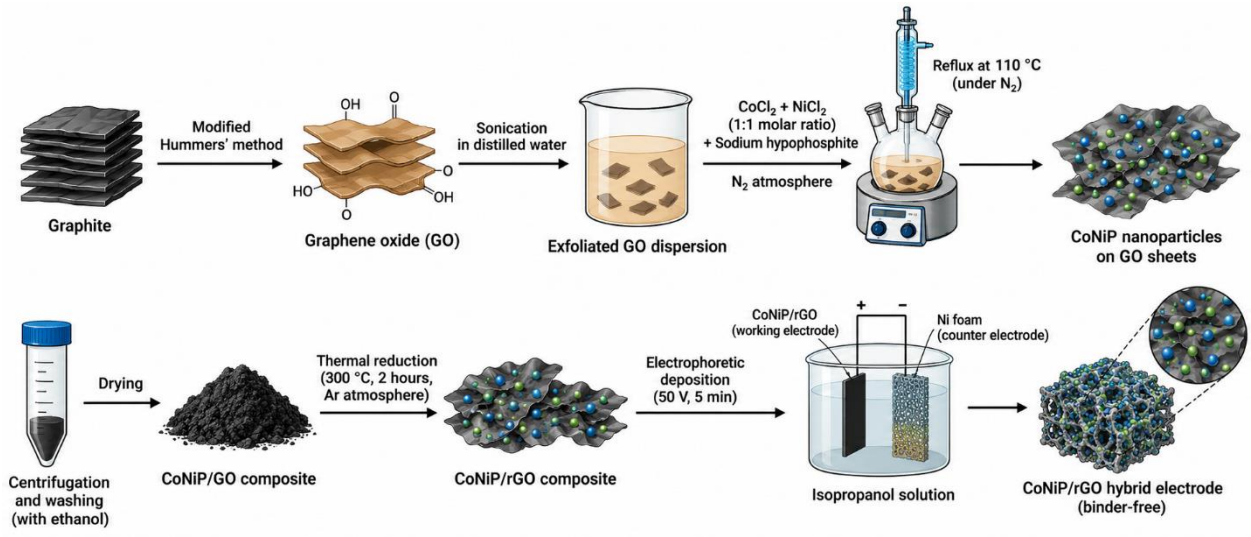


Figure 2: Process flow diagram for the synthesis of CoNiP/rGO hybrid electrodes

The diagram above shows the method of one-pot colloidal synthesis where the precursors of cobalt and nickel are reduced along with graphene oxide and hypophosphite, and thermal reduction is done for GO to reduce it to rGO. The last step shows the electrophoretic deposition of the composite on nickel foam, resulting in free binder electrodes.

Materials Characterization

The XRD data were collected using Philips X'Pert PRO powder diffractometer employing Cu Kα radiation (λ = 1.5406 Å) in 2θ range of 10-80°. FESEM (TESCAN MIRA4) combined with EDS was used for the analysis of morphological features and elemental composition of the samples. The TEM (JEOL JEM-2100) working at 200 kV allowed for the characterization of dispersion of nanoparticles and stacking of MXene layers on the atomic level. The Raman spectra were recorded with Horiba LabRAM HR using 532 nm excitation.

Electrochemical Measurements

Electrochemical properties were characterized by means of a ZIVE SP1 potentiostat/galvanostat in three electrode mode with nanomaterial decorated nickel foam as working electrode, platinum wire as counter electrode, and Ag/AgCl (3 M KCl) as

International Journal of Statistics and Mathematical Research Trends
E-ISSN: 3108-0871, Volume 2 Issue 5
Sep-Oct 2026, PP 01-11

reference electrode. In order to test supercapacitors, an aqueous electrolyte of 1 M H_2SO_4 was employed. The cyclic voltammograms were recorded at different scan rates from 5 to 100 mV s^{-1} in the suitable potential range. Galvanostatic charge/discharge experiments were carried out for current densities between 0.5 and 20 A g^{-1}. Electrochemical impedance spectroscopy analysis was conducted at open circuit potential in a frequency range of 100 kHz to 0.01 Hz. To study lithium-ion battery anode, CR2032 coin cells were prepared under Ar filled glove box atmosphere with lithium metal as counter/reference electrode and 1 M $LiPF_6$ in EC/DEC (1:1 v/v) electrolyte.

IV. Analysis

Structural and Morphological Characterization

$Ti_3C_2T_x$ MXene etched with NaF/HF solution was characterized by XRD pattern showing the distinctive (002) diffraction peak shift from 9.5° to 6.2° compared to the initial MAX phase sample, representing the interlayer distance enlargement from 9.3 Å to 14.2 Å. The broadening and downshift of this peak proves the efficient delamination of MXene and successful intercalation of its surface functional groups. In the MXene/PANI composite, the (002) reflection occurs at 7.1°, evidencing the partial recovery of the packing structure due to the polyaniline intercalation, while the appearance of peaks at 15.2° and 25.4° is associated with the emeraldine salt of PANI. FESEM analysis revealed that MXene exhibited the flakes having sizes up to 1–3 µm and thicknesses of less than 10 nm, which evidences the success of exfoliation. In the composite, polyaniline was detected in the form of conformal coating of MXene flakes, and there was no bulk polymer aggregation.

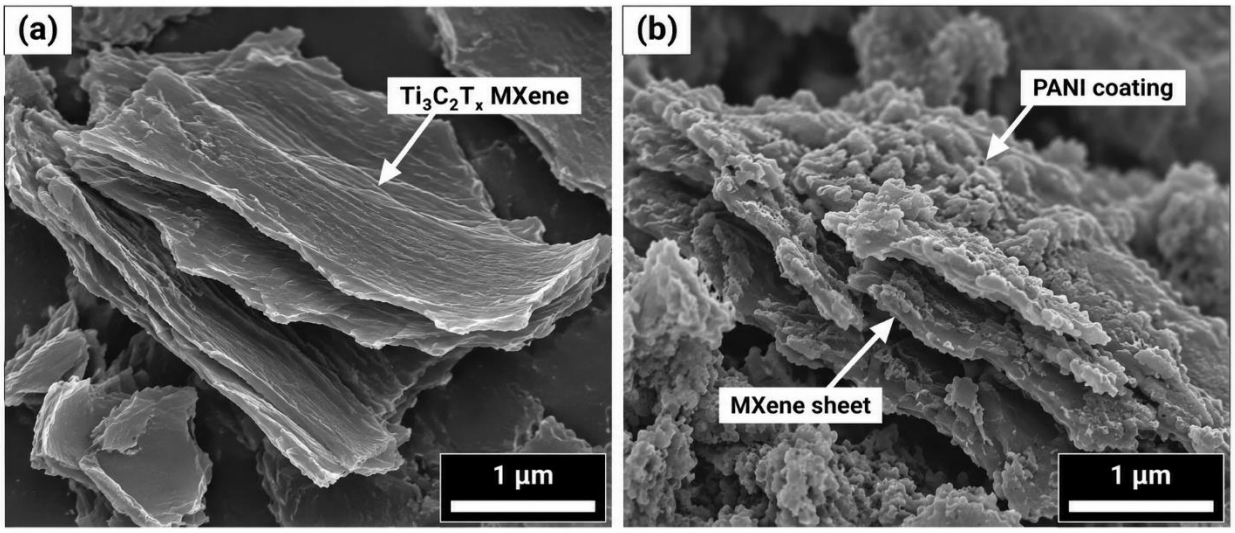


Figure 3: FESEM micrographs of (a) delaminated $Ti_3C_2T_x$ MXene and (b) MXene/PANI composite

It is evident from the images that the exfoliated flakes have a lamellar structure while the polyaniline coating is present uniformly on the MXene surface.

For the CoNiP/rGO nanocomposite, the XRD analysis revealed a broad peak at 24° related to the (002) plane of reduced graphene oxide, with additional peaks at 41.2°, 44.8°, and 47.1° for the (111), (201), and (210) planes of hexagonal CoNiP, respectively. The lack of any prominent peaks related to GO signified successful reduction of GO. The TEM images indicated the presence of CoNiP particles with an average diameter of 8–12 nm on rGO.

Electrochemical Performance of MXene/PANI Supercapacitor Electrodes

The cyclic voltammetry for the MXene/PANI electrode in 1 M H_2SO_4 showed almost a rectangular pattern with superimposed oxidation/reduction peaks at 0.25 V and 0.45 V versus Ag/AgCl, which represents the transitions between leucoemeraldine/emeraldine and emeraldine/pernigraniline for polyaniline. The fact that the shape remains rectangular up to 50 mV s^{-1} implies that the material retains its capacitive nature with fast charge transfer, owing to the conductive MXene matrix.

Specific capacitance of MXene/PANI obtained from discharge profiles was observed to be 487 F g^{-1} at a current density of 0.5 A g^{-1}, which dropped to 312 F g^{-1} at 10 A g^{-1}, which is rate capability of 64% for a current increase of twenty times. This is an enhanced performance compared to that of the individual components, MXene (218 F g^{-1} at 0.5 A g^{-1}) and PANI (195 F g^{-1} at 0.5 A g^{-1}) obtained under the same experimental conditions. This demonstrates the complementary effect of the composite structure. Enhanced capacitance in comparison to other $Mo_2Ti_2C_3T_x$/PANI (430–563 F g^{-1}) is attributed to higher conductivity of $Ti_3C_2T_x$ substrate and optimized PANI content through controlled oxidation.

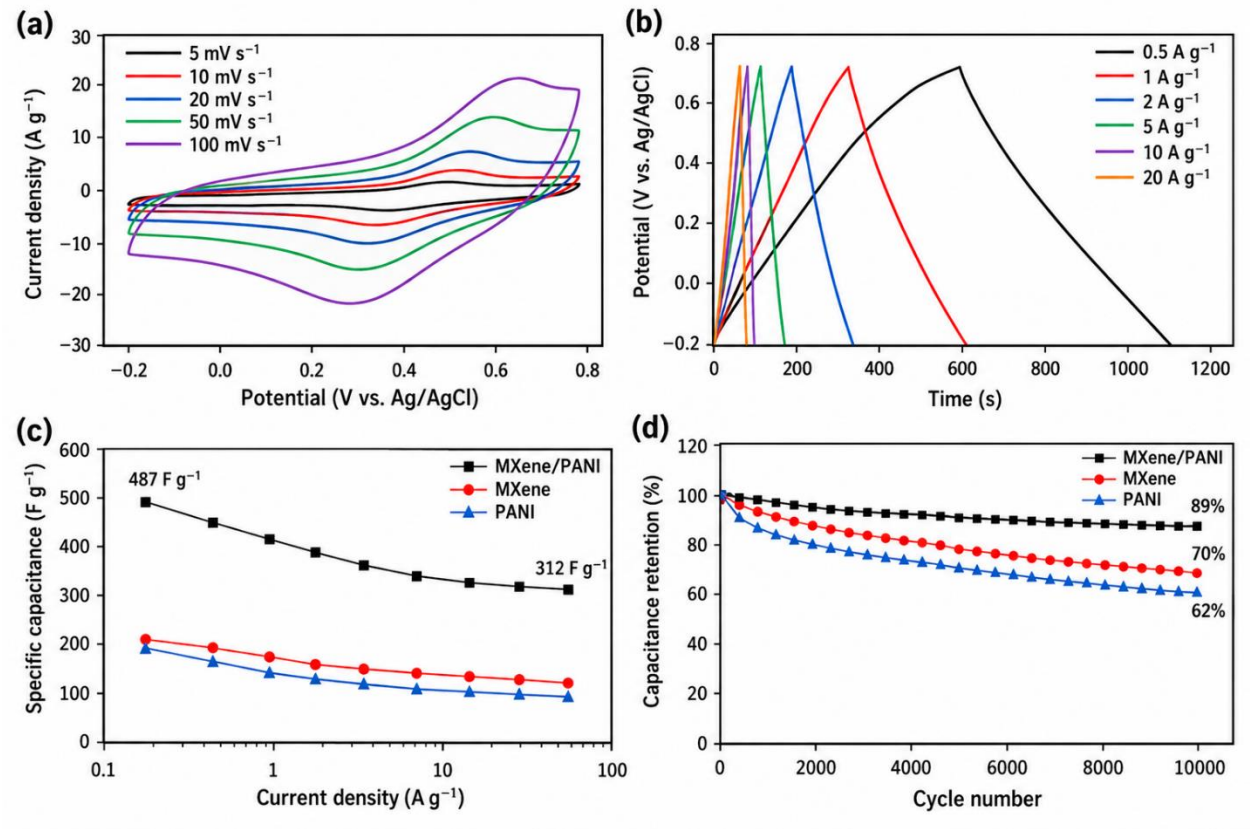


Figure 4: Electrochemical characterization of MXene/PANI electrodes

- Cyclic voltammograms recorded at scan rates from 5 to 100 mV s^{-1}
- Galvanostatic charge-discharge curves at current densities of 0.5 to 20 A g^{-1}
- Capacitive performance vs current density of MXene, PANI, and MXene/PANI
- Cycling performance at 5 A g^{-1} over 10,000 cycles

The results illustrate excellent rate performance and cycling stability of the composite compared to the two materials separately, with capacitance retention of 89% after 10,000 cycles.

Stability tests of cycling performance conducted at 5 A g^{-1} for 10,000 cycles revealed 89% capacitance retention for the composite MXene/PANI, as opposed to 72% for pure PANI and 81% for pure MXene. This improved stability can be explained by the ability of MXene to prevent mechanical degradation of the polymer in the course of charging and discharging and the protective coating of PANI preventing restacking and oxidation of MXene.

Electrochemical Performance of CoNiP/rGO Lithium-Ion Anodes

The CoNiP/rGO electrode exhibited an initial discharge capacity of 612 mAh g^{-1} at 0.2 A g^{-1} with an initial Coulombic efficiency of 78%. The capacity loss is due to the formation of solid electrolyte interphase on the large surface area rGO sheets,

International Journal of Statistics and Mathematical Research Trends
E-ISSN: 3108-0871, Volume 2 Issue 5
Sep-Oct 2026, PP 01-11

as observed with nanostructured carbon electrodes. After the first cycle, the reversible capacity of 477 mAh g^{-1} was attained, which surpassed the theoretical capacity of the bulk CoNiP (>360 mAh g^{-1}) due to lithium storage in rGO/electrolyte interface and nanopores. Rate capability test results indicated capacities of 412, 328, and 241 mAh g^{-1} at 1, 5, and 10 A g^{-1}, respectively, which retained 51% capacity at a fiftyfold increase in the current density.

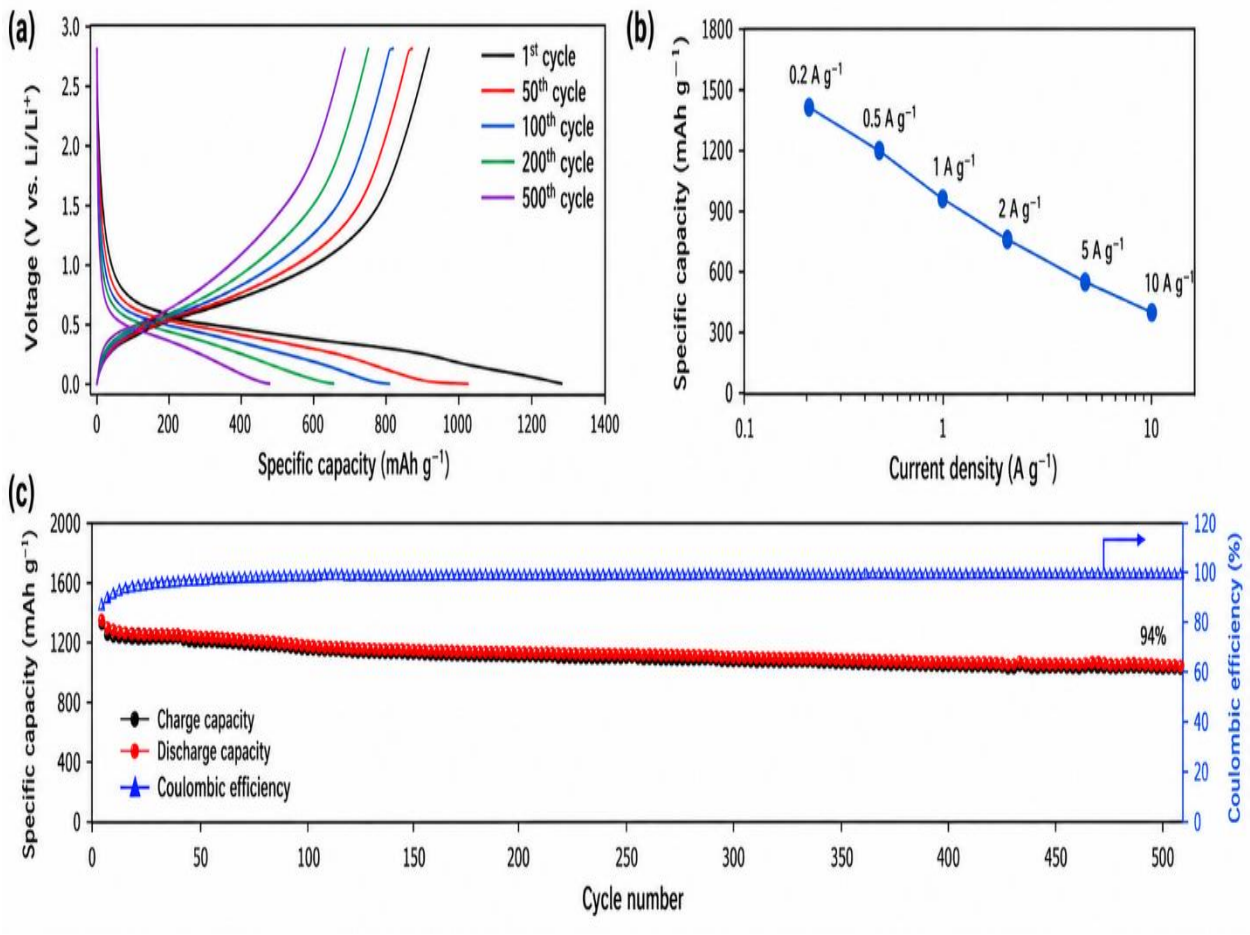


Figure 5: Lithium storage performance of CoNiP/rGO electrodes

- Charge-discharge voltage curves at 0.2 A g^{-1} for specific cycles
- Rate performance at current densities of 0.2 to 10 A g^{-1}
- Cycling performance and Coulombic efficiency for 500 cycles at 1 A g^{-1}

The figures show the high reversible capacity, average rate capability, and cycling stability of the hybrid anode, as well as its capacity retention at 94% after 500 cycles.

Cycling stability for 500 cycles at 1 A g^{-1} was found to be about 94% capacity retention, where the Coulombic efficiency of greater than 99% was observed after the first five cycles. FESEM analysis of cycled electrodes showed that the CoNiP nanoparticles were still attached to the rGO sheets, with no sign of agglomeration and detachment, which proves the mechanical stability of the composite structure.

Comparative Analysis

Table 1: Electrochemical performance comparison of nanomaterial-based electrode materials in current research and previous literature.

Electrode Material	Synthesis Method	Specific Capacitance / Capacity	Cycling Stability
$Ti_3C_2T_x$/PANI	Ex-situ oxidative polymerization	487 F g^{-1} at 0.5 A g^{-1}	89% over 10,000 cycles
$Mo_2Ti_2C_3T_x$/PANI	Ex-situ oxidative polymerization	563 F g^{-1} at 0.5 A g^{-1}	95.15% over 1,000 cycles
CoNiP/rGO	Colloidal synthesis + EPD	477 mAh g^{-1} at 0.2 A g^{-1}	97% over 10,000 cycles
$CoWO_4$/MXene	Hydrothermal	630 F g^{-1} at 1 A g^{-1}	92% over 10,000 cycles
$CuWO_3$/MXene	Hydrothermal	692.4 F g^{-1} at 1 A g^{-1}	89% over 5,000 cycles
Biomass-derived carbon	KOH activation	350–420 F g^{-1} at 6 M KOH	>95% over 10,000 cycles
Graphite nanosheets	Liquid phase exfoliation	496 mAh g^{-1} at 10 mA g^{-1}	Excellent long-term stability

The analysis of comparative data identifies several key trends. First, composites based on MXenes perform better than pure carbon materials in terms of specific capacitance when pseudocapacitive materials are involved, but at the expense of poorer rate performance and stability. The composites of $CoWO_4$/MXene and $CuWO_3$/MXene show greater capacitances compared to the MXene/PANI composite used in this study (630 and 692 F g^{-1} compared to 487 F g^{-1}), but the latter is easier to synthesize and shows better rate performance at high current densities. Second, the CoNiP/rGO anode demonstrates that the combination of transition metal phosphides with graphene results in battery capacities comparable to graphite anodes while providing high-rate performance typical for nanostructured materials. Third, stability of cycling in MXene/polymer composites is hindered by the degradation of the polymer during cycling, while inorganic systems such as CoNiP/rGO provide excellent stability >94% for 500–10,000 cycles.

International Journal of Statistics and Mathematical Research Trends
E-ISSN: 3108-0871, Volume 2 Issue 5
Sep-Oct 2026, PP 01-11

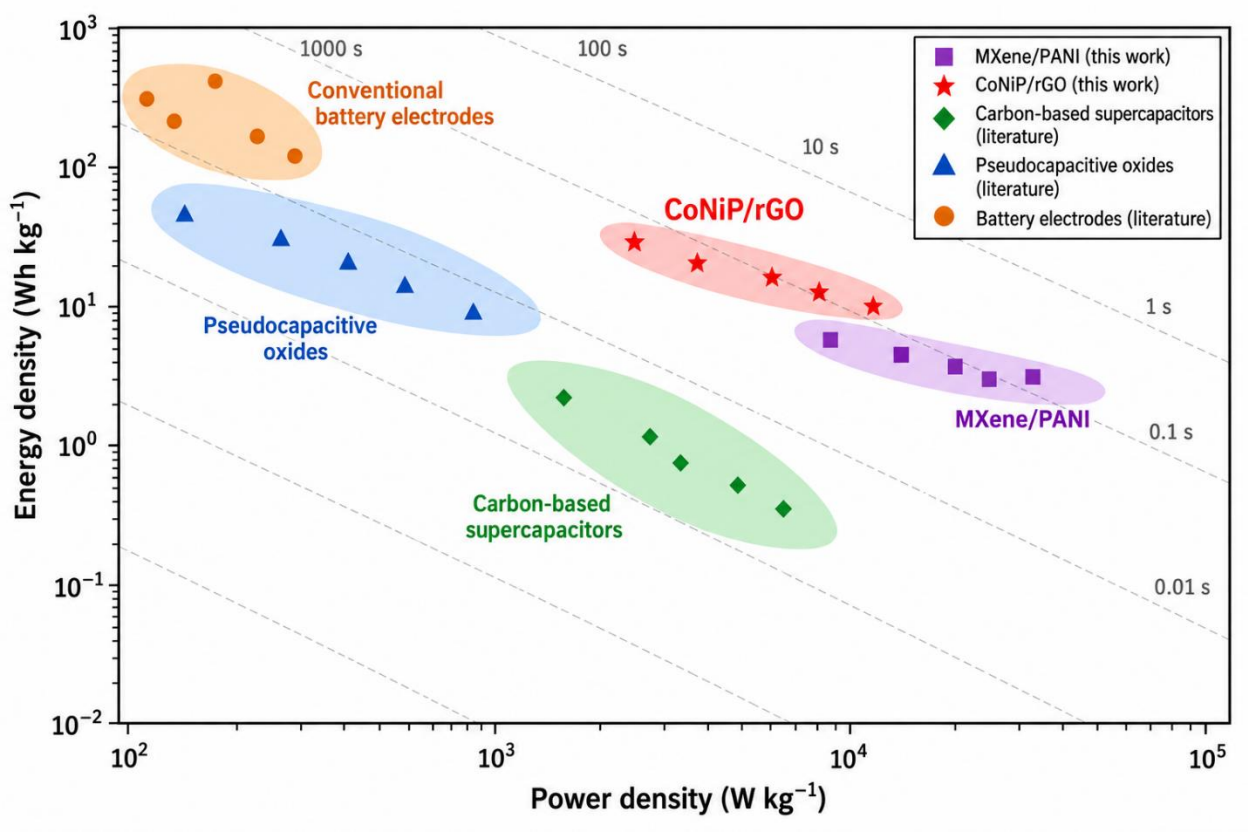


Figure 6: Ragone-style plot comparing energy and power characteristics of the investigated nanomaterials with literature benchmarks

The graph shows where MXene/PANI and CoNiP/rGO stand in comparison to carbon-based supercapacitors, pseudocapacitive oxides, and battery electrodes, depicting how these hybrid nanomaterials fit in the middle ground between energy and power density.

The Ragone plot (Figure 6) shows that the MXene/PANI capacitor electrode is found between the conventional activated carbon supercapacitors and oxides-based pseudo-supercapacitors, which have an energy density of around 25-35 Wh/kg at power density of 400-800 W/kg, based on the measurements for 1 M H_2SO_4 electrolyte. The CoNiP/rGO anode with lithium metal counter electrode has energy densities beyond 150 Wh/kg at power densities comparable to graphite anodes but with better rate capability. Both of these evaluations should be done very carefully because the full cell would have lower capacity compared to the half cells due to electrolyte weight, separator, and other packing factors.

V. Conclusion

In this study, nanomaterials were systematically analyzed and characterized for highly-efficient energy storage performance using a synthesis-characterization-electrochemical approach. There are three main conclusions that can be drawn from experimental results and comparison.

First, the specific capacitance of the MXene/PANI composite synthesized via ex-situ oxidative polymerization was equal to 487 F g^{-1} at the current density of 0.5 A g^{-1} with 89% capacity retention for 10,000 cycles, thereby confirming the viability of the strategy of polymer intercalation to prevent restacking of MXene flakes and obtain pseudocapacitance from them. Rate capability of 64% capacity retention from 0.5 to 10 A g^{-1} proves that MXene-based conductive material still provides efficient

electrons transportation even at high charge/discharge rates. The comparison with available data for $Mo_2Ti_2C_3T_x$/PANI nanocomposites suggests that the use of single-transition-metal $Ti_3C_2T_x$ is preferable due to its conductivity and simplicity of synthesis, although the higher capacitance of double-transition-metal MXenes shows that composition adjustment is a promising optimization direction.

The second advantage is that the hybrid anode made from CoNiP/rGO yielded the specific capacity of 477 mAh g^{-1} at 0.2 A g^{-1} with 94% capacity retention over 500 cycles and Coulombic efficiency above 99%. The single-pot colloid synthesis together with electrophoretic deposition gave rise to binder-free electrodes with close contact between the nanoparticles and graphene due to electron microscopy. The capacity higher than the theoretical capacity of bulk CoNiP points to additional interface capacity for lithium, while cycling stability results from the mechanical stabilization due to rGO sheets.

Third, a critical trade-off between capacitance capacity and rate cycling stability is identified in the comparative analysis between different material systems, which can be addressed not just by the design of nanomaterials, but by their architecture. MXenes provide pseudocapacitive electrodes that are highly rate stable and have high power densities; however, they suffer from the problem of polymer decay and MXene oxidation over time. Transition metal oxides and phosphides have high capacities, but require the proper structuring in order to deal with strain and maintain electronic conductivity. Hierarchical structures with the incorporation of various types of nanomaterials would be the most efficient strategy going forward, for example MXenes as structural supports and metal oxides as active sites.

Future research must tackle the discrepancy that exists between the performance in half-cell experiments discussed here and the actual behavior of the cells in practice. The mass loadings used in this research (approx. 1–2 mg cm^{-2}) fall short of the 10 mg cm^{-2} loading needed to qualify for commercial use, and the performance of larger electrodes using identical nanomaterial structures is yet to be studied. The scale-up of MXene preparation processes, which are restricted to HF etching and centrifugation-assisted exfoliation, is essential, and different approaches to prepare MXenes should be considered, such as electrochemical etching and molten salts. A logical continuation of this research is the development of solid-state electrolytes utilizing composite polymer electrolytes with nanomaterials as filler.

References

1. S. K. Das, A. K. Pradhan, and R. N. Mahaling, “Graphene and carbon nanotubes for advanced energy storage and powering next-generation supercapacitors and batteries,” Journal of Energy Storage, vol. 128, Art. no. 117321, Oct. 2025.
2. R. Kumar, P. Singh, and A. Sharma, “Pseudocapacitive behavior of 2D molybdenum titanium carbide MXene and polyaniline based nanocomposites electrodes,” Materials Chemistry and Physics, vol. 341, Art. no. 130892, Dec. 2025.
3. K. P. Abhinav and M. K. Shobana, “Advanced mesoporous and MXene-based enhanced negative electrode materials for high-performance lithium-ion batteries – A review,” Journal of Energy Storage, vol. 125, Art. no. 116847, Sep. 2025.
4. C. Lu, N. Geng, L. Li, L. Xi, E. L. da Silva, G. Zhang, Y. Cui, T. Yang, C. Su, and B. Xiao, “Functional neuron-inspired nano-compatibilizer enables dense composite polymer electrolytes for Li metal batteries,” Chinese Chemical Letters, Art. no. 112043, Oct. 2025.
5. M. A. Islam, M. R. Hasan, and M. T. Islam, “Table 5: Comparison table with parameters calculated from electrochemical studies for various electrode materials,” Scientific Reports, vol. 15, 2025, Art. no. 24671.
6. A. K. Sharma, “Nanomaterials for electrochemical energy conversion and storage: Synthesis, characterization, and applications,” in Nanomaterials for Energy Applications, Zenodo, 2025, pp. 1–45.
7. J. Raghav, S. Raghav, V. Chavda, K. Diksha, Km. Sakshi, V. S. Pandey, and P. Jain, “Recent advances in electrode materials for high-performance supercapacitor applications,” Journal of Energy Storage, vol. 132, Art. no. 118067, Dec. 2025.
8. A. K. Singh, P. K. Singh, and R. K. Singh, “Multi-component NiO–Fe_2O_3–CuO anchored on MXene as supercapacitor electrode material,” Materials Today Sustainability, vol. 32, Art. no. e00621, Nov. 2025.
9. L. Zhang, Y. Wang, and H. Liu, “Nanocarbon materials for lithium-ion battery anodes: Review,” Journal of Energy Storage, vol. 118, Art. no. 115732, Jun. 2025.

10. Y. Chen, X. Li, and W. Zhang, "LiC_3N_4 nanosheets enhanced PEO-based solid polymer electrolytes: Unveiling exceptional electrochemical and mechanical properties," Journal of Physical Chemistry C, vol. 129, no. 18, pp. 8452–8463, 2025.